Scientific paper

Nuclear Quadrupole Resonance Study of Hydrogen Bonded Solid Materials

Janez Seliger[1,2,3]

[1] »Jozef Stefan« Institute, Jamova 39, 1000 Ljubljana, Slovenia

[2] Faculty of Mathematics and Physics, University of Ljubljana, Jadranska 19, 1000 Ljubljana, Slovenia

[3] EN-FIST Centre of Excellence, Dunajska 156, 1000 Ljubljana, Slovenia

** Corresponding author: E-mail: janez.seliger@fmf.uni-lj.si*

Received: 31-03-2011

Dedicated to Professor Dušan Hadži on the occasion of his 90th birthday

Abstract

Nuclear quadrupole resonance is presented as a method for the study of solid hydrogen bonded materials. NQR study of hydrogen bonds in ferroelectric and paraelectric KH_2PO_4, antiferroelectric and paraelectric squaric acid, ferroelectric croconic acid and antiferroelectric and paraelectric cocrystal 5'-dimethyl-2,2'-bipyridine – chloranilic acid (1:1) are discussed in more details. A ^{14}N NQR study of the strong short O-H…N hydrogen bond in two polymorphic forms of cocrystal isonicotinamide-oxalic acid (2:1) is presented as well. Various correlations between the NQR parameters and between the NQR and structural parameters have been observed. These correlations may be used to determine the proton position in a hydrogen bond and some other structural parameters from the NQR data.

Keywords: Nuclear quadrupole resonance, hydrogen bond, ferroelectrics

1. Introduction

The hydrogen bond X-H…Y is an attractive interaction between the hydrogen bond donor X-H (O-H, N-H, ...) and an electronegative hydrogen bond acceptor Y (O, N, F ...). In solids hydrogen bonds influence molecular packing and conformation. Hydrogen bonds may be responsible for crystal polymorphism. Various macroscopic properties of solid materials, as for example melting point, solubility, ferroelectricity etc, may depend on hydrogen bonds. A strong and short hydrogen bond may represent a low barrier for the proton transfer from the hydrogen bond donor to the hydrogen bond acceptor. In such a case proton may exhibit a two site exchange across the barrier.

A quadrupole nucleus, ^2H, ^7Li, ^{14}N, ^{17}O, ^{23}Na, etc, has in addition to a nuclear magnetic moment also a nuclear electric quadrupole moment eQ. The interaction of a nuclear magnetic moments with an external magnetic field gives rise to the nuclear Zeeman energy levels. The transitions between the Zeeman energy levels are observed in NMR. The interaction of a nuclear electric quadrupole moment with the local inhomogeneous electric field, produced by the neighboring electric charges, gives in absence of external magnetic field rise to nuclear quadrupole energy levels. The transition frequencies between the nuclear quadrupole energy levels are named the nuclear quadrupole resonance (NQR) frequencies. They depend on two parameters: the quadrupole coupling constant e^2qQ/h and the asymmetry parameter η of the electric field gradient (EFG) tensor. The NQR frequencies are a sensitive test of the electric charge distribution around the observed nucleus. Even a small change in the electron charge distribution may result in measurable shifts of the NQR frequencies.

The most common quadrupole nuclei, found in the hydrogen bonds, are ^{14}N, ^{17}O and ^2H with the natural abundance 99,6%, 0.037% and 0.016% respectively. It is usually simple to deuterate a hydrogen bond, but the increase of the ^{17}O content is more complicated and more expensive.

In the continuation we present the basis of ^2H, ^{14}N and ^{17}O NQR, the techniques used to detect the NQR parameters and the application of NQR to the study of hydrogen bonded ferroelectrics and short strong hydrogen bonds.

2. ^{2}H, ^{14}N and ^{17}O NQR

The Hamiltonian H_Q, describing the interaction of a nuclear electric quadrupole moment with the external electric field, reads[1]

$$H_Q = \frac{eQ}{6I(2I-1)} \sum_{kl} V_{kl} \left[\frac{3}{2}(I_k I_l + I_l I_k) - \delta_{kl} \vec{I}^{2} \right] \quad (1)$$

Here eQ is the nuclear quadrupole moment, I is the spin of the nucleus. The EFG tensor V_{kl}, $V_{kl} = \partial^2 V/\partial x_k \partial x_l$, is composed of the second derivative of the electrostatic potential V with respect to the coordinates and I_k and I_l are the components of the nuclear spin operator $\vec{I}$. The traceless second rank EFG tensor is diagonal in the principal axis frame X, Y, Z. The principal axes are ordered so that $|V_{ZZ}| > |V_{YY}| \geq |V_{XX}|$. In the principal axis frame of the EFG tensor the Hamiltonian H_Q reads

$$H_Q = \frac{e^2qQ}{4I(2I-1)} \left[3I_z^2 - \vec{I}^2 + \frac{\eta}{2}(I_+^2 + I_-^2) \right] \quad (2)$$

Here eq is the largest principal value V_{ZZ} of the EFG tensor and eQ is the electric quadrupole moment of the nucleus. The ratio $e^2qQ/h = eQV_{ZZ}/h$, where h Is the Planck constant, is called the quadrupole coupling constant and $\eta = (V_{XX} - V_{YY})/V_{ZZ}$ is the asymmetry parameter of the EFG tensor, which ranges between 0 and 1. The quadrupole coupling constant can be either positive or negative, depending on the signs of eq and eQ. The sign of e^2qQ/h can not be determined by a NQR experiment.

The nuclear isotopes ^{2}H and ^{14}N have both spin I = 1. They have in zero magnetic field three generally non-degenerated quadrupole energy levels. Their energies can be calculated from Expression (2). The three transition (NQR) frequencies between these energy levels, labeled as ν_+, ν_- and ν_0, are equal

$$\begin{aligned} \nu_+ &= \frac{e^2qQ}{4h}(3+\eta) \\ \nu_- &= \frac{e^2qQ}{4h}(3-\eta) \\ \nu_0 &= \nu_+ - \nu_- = \frac{e^2qQ}{2h}\eta \end{aligned} \quad (3)$$

The quadrupole coupling constant e^2qQ/h is calculated from the sum $\nu_+ + \nu_-$ and then the asymmetry parameter η is obtained as $\eta = 2\nu_0/(e^2qQ/h)$. The ^{14}N NQR frequencies are mainly lower than 5MHz and the ^{2}H NQR frequencies are of the order of 100 kHz

The nuclear isotope ^{17}O has a spin I = 5/2. In zero magnetic field it exhibits three doubly degenerated nuclear quadrupole energy levels. Their energies E_i are obtained as the solutions x_i of the secular equation

$$x^3 - 7(3+\eta^2)x - 20(1-\eta^2) = 0 \quad (4)$$

multiplied by $e^2qQ/20$, $E_i = e^2qQx_i/20$. The resonance, NQR, frequencies are calculated as the differences of these energies divided by the Planck constant h. The ^{17}O NQR frequencies are labeled as $\nu_{5/2-1/2} > \nu_{5/2-3/2} \geq \nu_{3/2-1/2}$. They uniquely depend on the quadrupole coupling constant e^2qQ/h and the asymmetry parameter η, that are from the measured NQR frequencies calculated in the following way. First the asymmetry parameter η is determined from the ratio $R = \nu_{3/2-1/2}/\nu_{5/2-3/2}$, which monotonously varies from R = 0.5 at $\eta = 0$ to R = 1 at $\eta = 1$. When η is known, the quadrupole coupling constant is calculated from any NQR frequency. The ^{17}O NQR frequencies $\nu_{5/2-3/2}$ and $\nu_{3/2-1/2}$, which are easier to detect than $\nu_{5/2-1/2}$, are mainly lower than 5 MHz. The resonance frequency $\nu_{5/2-1/2}$ can not always be detected. The matrix element for this transition is zero when $\eta = 0$ and remains small even for large values of η.[2]

3. The Measurement of the NQR Parameters

The NQR parameters e^2qQ/h and η of ^{2}H are usually measured by quadrupole perturbed NMR. When the sample is in a high magnetic field, the nuclear quadrupole interaction (Expression (1)) perturbes the Zeeman interaction in the first order and splits a NMR line into a doublet. In a powder sample the nuclear quadrupole interaction produces a frequency distribution. The shape and the width of the frequency distribution are used to determine e^2qQ/h and η.

In case of ^{17}O there are two possibilities. The frequency distribution of the central, –1/2 – 1/2, NMR transition, as measured under magic angle spinning, can be used to determine the two NQR parameters in powders. Sometimes it is more convenient to measure the ^{17}O NQR frequencies by double resonance and determine e^2qQ/h and η from the NQR frequencies. The advantage of double resonance is its high sensitivity. In addition in case of a short ^{17}O-^{1}H distance the dipolar structure of the ^{17}O NQR lines reflects the O-H distance, the orientation of the O-H bond in the principal axes frame of the EFG tensor and the sign of the quadrupole coupling constant.

The ^{14}N NQR parameters are mainly not measured by NMR. The ^{14}N quadrupole perturbed NMR lines are usually several MHz broad and the magnetic moment of ^{14}N is low. Pulse NQR and various double resonance techniques are used to measure the ^{14}N NQR frequencies

Nuclear quadrupole double resonance (NQDR) is an indirect method of detection of the quadrupole nuclei via their influence on the proton NMR signal. NQDR is based on magnetic field cycling. A magnetic field cycle is schematically represented in Figure 1.

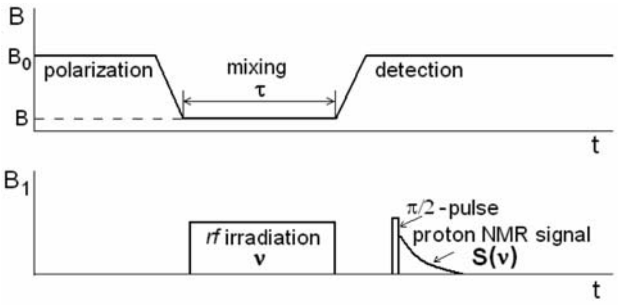

Figure 1. Schematic presentation of a magnetic field cycle.

The proton spin system is first polarized in the high static magnetic field B_0. The sample is then transferred to a second magnet, where the magnetic field B is much lower than B_0. The spin temperature of the proton spin system reduces by a factor of B/B_0. The sample is during the mixing phase irradiated with a radiofrequency (*rf*) magnetic field with the frequency ν. When the frequency ν is close to a NQR frequency, the energy is via the dipole-dipole interaction transferred from the quadrupole spin system to the "cold" proton spin system. This energy increases the proton spin temperature and reduces the proton NMR signal S at the end of the magnetic field cycle, when the sample is transferred back into the first magnet.

Several NQDR techniques are used to detect the quadrupole nuclei under various experimental conditions. The ^{17}O NQR frequencies are usually measured by the Slusher and Hahn's technique.[3] The dipolar structures of the ^{17}O NQR lines are resolved by double resonance with coupled multiplets[4] and a method of analysis of the dipolar structures is presented in reference.[5] The ^{14}N and ^{2}H NQR frequencies may be measured by the cross relaxation spectroscopy,[6–8] level crossing technique,[9,10] solid effect technique[11,12] and by the technique using multiple frequency sweeps of the *rf* magnetic field and two-frequency irradiation.[13,14]

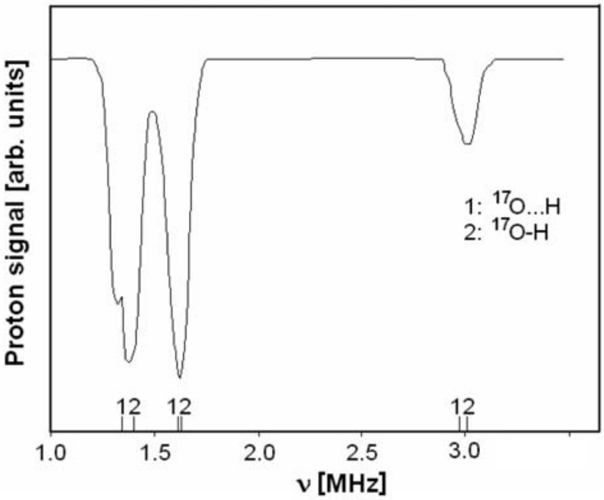

Figure 2. ^1H-^{17}O NQDR spectrum of benzoylacetone at T = 173 K as measured by the Slusher and Hahn's technique. The ^{17}O NQR frequencies, as determined by double resonance with coupled multiplets, are labeled and shown as sticks on the frequency scale

An illustrative NQDR spectrum is presented in Figure 2. It is the ^1H-^{17}O NQDR spectrum of benzoylacetone as measured by the Slusher and Hahn's technique.

4. Hydrogen Bonded Materials

4. 1. KH_0PO_4

KH_2PO_4 is perhaps the most studied hydrogen bonded ferroelectric crystal. A PO_4 groups is in a KH_2PO_4 crystal linked to four other PO_4 groups by the O-H…O hydrogen bonds. The hydrogen bonds are in the paraelectric phase symmetric and disordered. A proton is exchanging between two equivalent equilibrium positions O-H…O and O…H-O in a hydrogen bond. Below the Curie temperature T_C the exchange freezes and a polar ferroelectric order occurs.

^{17}O NQR spectrum[15, 16] shows in the paraelectric phase three resonance lines belonging to a single oxygen position. All oxygen positions in the unit cell are thus crystallographically equivalent in agreement with the crystal structure and the symmetry of the hydrogen bonds. This NQR spectrum also shows that the proton exchange is fast on the NQR (MHz) frequency scale so that the NQR spectrum is determined by the time-averaged EFG tensor. Below T_C each NQR line splits nearly symmetrically into two lines. One set of three lines corresponds to the ^{17}O-H…O oxygen position and the second set corresponds to the O-H…^{17}O oxygen position. A nearly symmetric splitting indicates that the EFG tensor observed in the paraelectric phase is indeed an average of the two EFG tensors observed in the ferroelectric phase. A NQDR measurement of the O-H distances in the paraelectric and ferroelectric phase [17] unambiguously shows the presence of the proton two-site exchange. The experimentally determined O-H distance R_{exp} is namely given as

$$\frac{1}{R_{exp}^3} = \left\langle \frac{1}{R^3} \right\rangle = \frac{1}{2}\left(\frac{1}{R_{O-H}^3} + \frac{1}{R_{O...H}^3} \right) \tag{5}$$

This distance is in case of a two-site exchange shorter than $R_{O...O}/2$.

A further analysis of the ^{17}O NQR data in systems containing P-O-H…O=P hydrogen bonds[18] has shown that the principal values of the quadrupole coupling tensor at both the P-O-H and P=O…H oxygen positions correlate as

$$\begin{aligned} eQV_{XX}/h &= 2.65\,MHz - 0.33eQV_{YY}/h \\ eQV_{ZZ}/h &= -2.65\,MHz - 0.67eQV_{YY}/h \end{aligned} \tag{6}$$

The principal axis Y points nearly perpendicular to either the P-O-H or the P=O…H plane, as determined by double resonance with coupled multiplets.[4,5] This plane represents a local mirror plane for the electron distribution around the oxygen atom. The orientation of the in-plane principal axes X and Z with respect to the P-O bond may in principle vary when the strength of the hydrogen bond changes, but the nearly linear correlation (Expression 6) suggests that this variation is weak.

The principal value eQV_{YY}/h correlates also with the phosphorous-oxygen distance R_{PO} at both the P-O and P=O oxygen positions as

$$eQV_{YY}/h = 3.25\,MHz + 253(R_{PO} - 0.15nm)\,MHz/nm \quad (7)$$

The distance R_{PO} reflects the double bond character of the phosphorous-oxygen chemical bond and may be related to the strength oh the hydrogen bond formed by the oxygen atom.

It has long been known that the deuterium quadrupole coupling constant in the O-H…O hydrogen bonds strongly correlates with the bond length *R*(O…O).[19–21] The relationship proposed by Soda and Chiba[20] and modified by Poplett and Smith[21] reads

$$\frac{e^2qQ}{h} = 442.7kHz - \frac{4.882\,kHz(nm)^3}{R^3(O...O)} \quad (8)$$

The quadrupole coupling constant decreases with decreasing oxygen-oxygen distance *R*(O…O). A study of ^2H quadrupole coupling constant in partially deuterated KH_2PO_4[22] has shown that the length of the O-D…O bonds and presumably also the length of the O-H…O bonds increases linearly with increasing deuterium concentration what may influence the transition temperature T_C which also linearly increases with increasing deuterium concentration.

4. 2. Croconic Acid and Squaric Acid

The oxocarbon acids with the general formula $H_2C_nO_n$ are strongly acidic and form strong O-H…O hydrogen bonds in the solid state.

Croconic acid (4,5-dihydroxy-4-cyclopentene-1,2,3-trione, n = 5) was recently found to have a hydrogen bonded polar structure in the solid state.[23] The application of an electric field coherently aligns the molecular dipole moments in crystalline croconic acid and produces a well defined polarization at room temperature. The polarization can be switched by an electric field thus producing a well defined hysteresis loop characteristic of a ferroelectric. This molecular crystal exhibits, in spite of its small molecular size, the highest spontaneous polarization of all organic ferroelectrics, which persists up to more than 400 K.[24]

The crystal structure of squaric acid (3,4-Dihydroxycyclobut-3-ene-1,2-dione, n = 4) consists at room temperature of ordered layers of C_4O_4 groups. Each C_4O_4 group is linked to four neighboring C_4O_4 groups by the O-H…O hydrogen bonds. The layers are ferroelectrically ordered but antiferroelectrically stacked so that the dipole moments of adjacent layers are antiparallel.[25, 26] Squaric acid undergoes an antiferroelectric phase transition at $T_C \approx 374$ K, whereas in its fully deuterated analog T_C is shifted to 516 K. The upward shift of T_C on deuteration is a characteristic of the hydrogen bonded ferroelectrics.

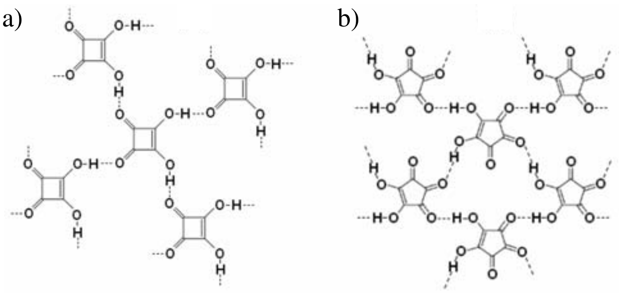

Figure 3. Hydrogen bonded layers of molecules in antiferroelectric squaric acid (a) and ferroelectric croconic acid (b).

The hydrogen bonded layers of croconic and squaric acid are presented in Figure 3**.** The lengths of the O-H…O hydrogen bonds are in croconic acid equal 2.628 Å and 2.617 Å. The hydrogen bonds are in squaric acid shorter, $R_{O...O} = 2.554$ Å.

^1H-^{17}O NQDR shows in squaric acid at room temperature the presence of two oxygen positions, ^{17}O-H…O and O-H…^{17}O, with the quadrupole coupling constants –7.6 MHz and 7.3 MHz respectively. The O-H distance is equal (1.03 ± 0.02)Å.[27] A single oxygen position is observed above T_C with the ^{17}O quadrupole coupling constant equal to ±6.2 MHz. The temperature dependence of the ^{17}O quadrupole coupling tensor has been analyzed in the model of two-site proton exchange. A good agreement between the experimental results and the results of the model calculations suggests that a proton indeed exchanges between two non-equivalent equilibrium positions below T_C and between two equivalent equilibrium positions above T_C.

In croconic acid five oxygen positions have been observed at room temperature by ^1H-^{17}O NQDR: two O-H positions with the quadrupole coupling constants –7.86 MHz and –7.92 MHz, two O…H positions with the quadrupole coupling constants 8.94 MHz and 9.73 MHz and the non hydrogen bonded oxygen position with the quadrupole coupling constant 10.16 MHz. [28]

The O-H distance is in both hydrogen bonds equal (0.98 ± 0.01) Å, what is unusually short for the hydrogen bonds with the length 2.62 Å.

A correlation between the O…O distance and the ^{17}O quadrupole coupling constant at the donor and acceptor positions has been observed in several organic acids forming the C-O-H…O=C hydrogen bonds: [28]

$$e^2q(O-H)Q/h = -10.7\ MHz + 0.06 MHz(nm)^3 / R(O...O)^3 \quad (9)$$

The data for croconic acid deviate from the correlation curves. The long range ferroelectric order in croconic acid seems to increase the energy difference of the two proton positions in a hydrogen bond and makes the hydrogen bonds more asymmetric than in non-ferroic hydrogen-bonded systems with comparable O…O distances.

The contribution of protons in the O-H…O hydrogen bonds to the spontaneous polarization P_s of croconic acid has been estimated as being about 1/3 of P_s.

4. 3. 5,5'-dimethyl-2,2'-bipyridine – chloranilic acid (1:1)

The 1:1 cocrystal of 5,5'-dimethyl-2,2'-bipyridine and chloranilic acid belongs to the group of the two-component compounds with the chloranilic acid acting as the hydrogen bond donor. The two types of molecules are alternately bound by one-dimensional chains of hydrogen bonds.[29] The compound undergoes an antiferroelectric phase transition at T_C = 318 K. In the high-temperature paraelectric phase the two types of molecules form bifurcated hydrogen bonds with a single-minimum proton potential, as presented in Figure 4. On going into the low-temperature antiferroelectric phase protons displace from their paraelectric positions, as shown by arrows in Figure 4, and the molecules are bound by the O-H…N and N^+-H…O^- hydrogen bonds. The hydrogen bonded chains are in the low temperature phase polar. The antiferroelectric phase is the consequence of two types of hydrogen bonded chains polarized in the opposite directions.

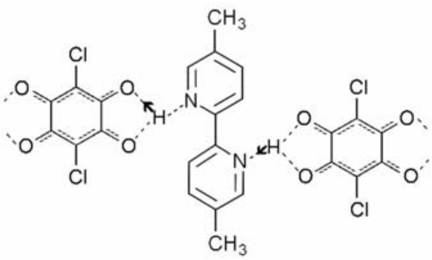

Figure 4. Positions of protons in the bifurcated hydrogen bonds in paraelectric 5,5'-dimethyl-2,2'-bipyridine – chloranilic acid (1:1). The displacement of protons on going into the antiferroelectric phase is indicated by arrows.

In the paraelectric phase there is a single triplet of the ^{14}N NQR frequencies (ν_+, ν_-, ν_0) observed showing the equivalency of the two nitrogen positions in a molecule.[30] The two nitrogen positions become non-equivalent in the antiferroelectric phase where two triplets of the ^{14}N NQR frequencies are observed. We may in the first order assume that the shift of a ^{14}N quadrupole coupling constant is proportional to the displacement of proton, which is bound to the nitrogen atom, from its paraelectric position. The shift of the ^{14}N quadrupole coupling constant is under this assumption proportional to the local order parameter S, which -according to the NQR data- varies close to T_C as $S \propto (T_C - T)^\beta$, where $\beta = 0.17$.

A correlation of the principal values of the ^{14}N quadrupole coupling tensor in 5,5'-dimethyl-2,2'-bipyridine are observed in the whole range from the non hydrogen bonded molecule (N) through the hydrogen bonded region (N…H) to the proton transfer (N^+-H) region. This correlation may be expressed as

$$\begin{aligned} eQV_{XX}/h &= 0.72\ MHz - 0.18 eQV_{ZZ}/h \\ eQV_{YY}/h &= -0.72\ MHz - 0.82 eQV_{ZZ}/h \end{aligned} \quad (10)$$

The ^{14}N quadrupole coupling constant is for the non hydrogen bonded molecule around –4.5 MHz, whereas it drops in case of proton transfer to around –1.1 MHz. The ^{14}N quadrupole coupling constant observed in the paraelectric phase is approximately in the middle of this region. The two ^{14}N quadrupole coupling constants observed in the antiferroelectric phase shift from the paraelectric value in the opposite directions: one towards the N limit and another towards the N^+-H limit. The shifts increase on decreasing temperature as the local order parameter increases.

Expressions (10) are characteristic for bipyridine. As we show later, we obtain slightly different correlation expressions for pyridine.

4. 4. Isonicotinamide – Oxalic Acid (2:1)

The cocrystals of isonicotinamide-oxalic acid (2:1) are composed of chains of hydrogen bonded pairs of isonicotinamide molecules "glued" by the oxalic acid molecules.[31,32,33] Two polymorphic forms of the isonicotinamide-oxalic acid (2:1) cocrystals are presented in Figure 5.

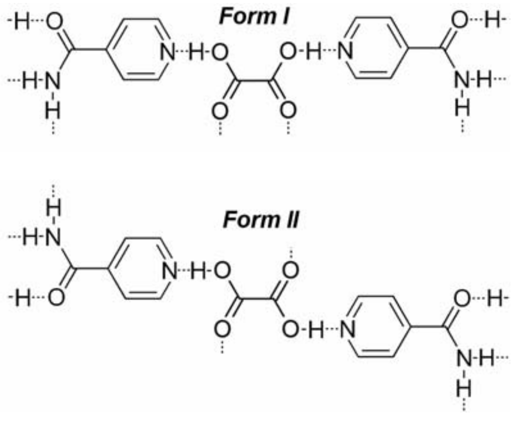

Figure 5. Hydrogen bonded chains of isonicotinamide and oxalic acid molecules in the two polymorphic forms of isonicotinamide-oxalic acid (2:1).

They differ in the cis-trans isomerism of the oxalic acid hydroxyl groups. The chains are cross-linked by further moderate strength N-H…O hydrogen bonds, forming a three-dimensional network in form I and a two-dimensional layered structure in form II. The O-H…N hydrogen bonds between the oxalic acid molecules and the ring nitrogen atoms of the isonicotinamide molecules are very short: 2.559 Å in form I and 2.539 Å in form II. Also the position of hydrogen in a O-H…N hydrogen bond is well displaced towards the center of the hydrogen bond in comparison to a isolated hydroxyl group, where the O-H distance is about 0.98 Å. The O-H and H…N distances are in the form I 1.161 Å and 1.398 Å respectively, while they are in the form II 1.235 Å and 1.313 Å respectively. The neutron diffraction data indicate no pronounced proton intrabond dynamics in any of the two phases.[31, 32]

The NQDR measurements[34] have shown in each form the presence of two nonequivalent nitrogen positions: the amide nitrogen position and the nitrogen position in the pyridine ring.

A correlation of the principal values of the ^{14}N quadrupole coupling tensor in hydrogen bonded pyridine has been observed in a broad range, covering non hydrogen bonded pyridine and even pyridine in the gas phase on one side and the pyridinium (N^+-H) ion on the other side. The correlation may be expressed as

$$\begin{aligned} eQV_{XX}/h &= 1.0\,MHz - 0.088 eQV_{ZZ}/h \\ eQV_{YY}/h &= -1.0\,MHz - 0.912 eQV_{ZZ}/h \end{aligned} \tag{11}$$

The ^{14}N quadrupole coupling constant in a non hydrogen bonded pyridine is around –4.6 MHz. On increasing hydrogen bond strength the quadrupole coupling constant decreases by magnitude. It should be noted that at $eQV_{ZZ}/h \approx -2.4$ MHz the principal values V_{XX} and V_{YY} cross and below this value the axes X and Y exchange. The labels X, Y and Z used in Expression (11) correspond to the principal axes of the ^{14}N EFG tensor in a non hydrogen bonded pyridine. At $eQV_{ZZ}/h \approx -1.1$ MHz V_{YY} passes zero and below this value the principal value V_{XX} is the largest by magnitude. The lowest absolute value of eQV_{ZZ}/h observed in case of an pyridinium ion is around 0. The ^{14}N quadrupole coupling constants at the ring nitrogen position in forms I and II are –2.605 MHz and 2.355 MHz respectively. Both values are close to the middle of the region of observed ^{14}N quadrupole coupling constants in agreement with the position of proton. The values of eQV_{XX}/h and eQV_{YY}/h in both forms strongly deviate from the correlation lines (Expression (11)). The deviation has been analyzed in a model assuming an excess electric charge on the nitrogen atom. The excess electric charge was obtained negative in both phases, so the hydrogen bonds seem to be of the type N^-. . .H-O. The attraction between the negative electric charge on the nitrogen atom and proton may influence the proton position in the hydrogen bond.

5. Conclusions

NQR is discussed as a tool for the study of hydrogen bonded solid materials. Some basic fundamentals of NQR are presented. The basic structural parameter, which can be directly measured by NQR, is the O-H distance. Various correlations between the NQR and structural parameters, as for example the correlation between the O-^{2}H…O distance and the ^{2}H quadrupole coupling constant, the correlation between the O-H…O distance and the ^{17}O-H…O and O-H…^{17}O quadrupole coupling constants and the correlation between the P-O distance and the ^{17}O quadrupole coupling constant, have been experimentally observed. These correlations are useful for a fast estimate of the structural data from the NQR parameters.

Correlations between the principal values of the ^{14}N quadrupole coupling tensor have been observed at the nitrogen position in pyridine and 5,5'-dimethyl-2,2'-bipyridine in the broad range from the non hydrogen bonded nitrogen through the range of hydrogen bonded nitrogen to the proton transfer (N^+-H) limit. These correlations are useful for the determination of the proton position in a hydrogen bond. A deviation from the correlation relations may be in this case the consequence of a redistribution of the electron electric charge within the molecule, as for example in isonicotinamide-oxalic acid (2:1) where approximately 20% of the electron electric charge is transferred from the amide nitrogen to the pyridine nitrogen. [34]

The data derived from the correlation relations are only the first step in understanding the crystal structure and hydrogen bonds. A more thorough analysis, as for example the DFT calculations, is needed to confirm the data obtained on the basis of simple arguments from the NQR spectra.

6. References

1. J. Seliger in: Encyclopedia of Spectroscopy and Spectrometry, J. C. Lindon, G. E. Tranter, J. L. Holmes (Eds.), Academic Press, San Diego etc., **2000**, pp. 1672–1680.
2. J. Seliger, V. Žagar, *J. Magn. Reson.* **2008,** *194,* 175–181.
3. R. E. Slusher, E. L. Hahn, *Phys. Rev*. **1968**, *166,* 332–347.
4. S. G. P.Brosnan, D. T. Edmonds, *J. Magn. Reson*. **1981**, *45,* 440–450.
5. J. Seliger, V. Žagar, R. Blinc, A. Novak, *J. Chem. Phys*. **1986**, *84,* 5857–5861.
6. J. Seliger, R. Osredkar, M. Mali, R. Blinc, *J. Chem. Phys*. **1976**, *65,* 2887–2891.
7. J. Seliger, R. Blinc, H. Arend, R. Kind, *Z. Phys. B,* **1976**, *25,* 189–195.
8. D. Stephenson, J. A. S. Smith, *Proc. Roy. Soc. A* **1988**, *416,* 149–178.
9. R. Blinc, M. Mali, R. Osredkar, A. Prelesnik, J. Seliger, I. Zupancic, L. Ehrenberg, *J. Chem. Phys.* **1972**, *57,* 5087–5093.

10. D. T. Edmonds, *Phys. Rep.* **1977**, *29,* 234–290.
11. J. Seliger, V. Žagar, *J. Magn. Reson.* **2008**, *193,* 54–62.
12. J. Seliger, R. Blinc, M. Mali, R. Osredkar, A. Prelesnik, *Phys. Rev. B* **1975,** *11,* 27–36
13. J. Seliger, V. Žagar, R. Blinc, *J. Magn. Reson. A* **1994**, *106,* 214–222.
14. J. Seliger, V. Žagar, R. Blinc, *Z. Naturforsch. A* **1994,** *49,* 31–34 .
15. R. Blinc, J. Seliger, R. Osredkar, T. Prelesnik, *Chem. Phys. Lett.* **1973,** *23,* 486–488.
16. R. Blinc, J. Seliger, R. Osredkar, M. Mali, *Phys. Lett. A* **1974,** *47,* 131–132.
17. S. G. P. Brosnan, D. T. Edmonds, *Phys. Lett. A* **1981**, *81*, 243–245.
18. J. Seliger, V. Žagar, *Magn. Reson. Chem*., 2008, *46,* 969–973
19. R. Blinc, D. Hadži, *Nature* **1966**, *212,* 1307–1309.
20. G. Soda, T. Chiba, *J. Chem. Phys*. **1969**, *50,* 439–445.
21. I. J. F. Poplett, J. A. S. Smith, *J. Chem. Soc., Faraday Trans. 2* **1978**, *74,* 1077–1087.
22. J. Seliger, V. Žagar, *Phys. Rev. B* **1999**, *59,* 13505–13508.
23. D. Braga, L. Maini, F. Grepioni, *CrystEngComm* **2001**, *6,* 1–3.
24. S. Horiuchi, Y. Tokunaga, G. Giovanetti, S. Picozzi, H. Itoh, R. Shimano, R. Kumai,Y. Tokura, *Nature* **2010**, *463,* 789–792.
25. D. Semmingsen, F. J. Hollander, T. F. Koetzle, *J. Chem. Phys.* **1977**, *66,* 4405–4412
26. Y. Wang, G. D. Stucky, J. M. Williams, *J. Chem. Soc. Perkin. Trans*. 1974, *11,* 35–27.
27. J. Seliger, V. Žagar, R. Blinc, *J. Magn. Reson*. **1984**, *58,* 359–369.
28. J. Seliger, J. Plavec, P. Šket, V. Žagar, R. Blinc, *Phys. Status Solidi B* **2011**, *248,* 2091-2096.
29. R. Kumai, S. Horiuchi, Y. Okimoto, Y. Tokura, *J. Chem. Phys*. **2006**, *125,* 084715.
30. J. Seliger, V. Žagar, T. Asaji, K. Gotoh, H. Ishida, *Phys. Chem. Chem. Phys*. **2011**, *13,* 9165–9172.
31. M. Schmidtmann, L. J. Farrugia, D. S. Middlemiss, M. J. Gutmann, G. J. McIntyre, C. C. Wilson, *J. Phys. Chem. A* **2009**, *113*, 13985–13997.
32. M. Schmidtmann, M. J. Gutmann, D. S. Middlemiss, C. C. Wilson, *CrystEngComm* **2007**, *9*, 743–745.
33. P. Vishweshwar, A. Nangia, V. M. Lynch, *Cryst. Growth Des.* **2003**, *3*, 783–790.
34. J. Seliger, V. Žagar, *J. Phys. Chem. A* **2010**, *114,* 12083–12087.

Povzetek

Članek predstavlja jedrsko kvadrupolno resonanco kot metodo za preučevanje trdnih materialov z vodikovimi vezmi. V podrobnostih predstavlja študij vodikovih vezi z jedrsko kvadrupolno resonanco v feroelektričnem in paraelektričnem KH_2PO_4, antiferoelektrični in paraelektrični kvadratni kislini, feroelektrični krokonski kislini ter antiferoelektričnem in paraelektričnem kokristalu 5’-dimetil-2,2’-bipiridin – kloranilna kislina (1:1). Članek predstavlja tudi študij močnih kratkih vodikovih vezi O–H...N v dveh polimorfnih formah kokristala izonikotinamid – oksalna kislina (2:1) z jedrsko kvadrupolno resonanco ^{14}N. Rezultati meritev kažejo korelacije med parametri jedrske kvadrupolne resonance in strukturnimi parametri, ki jih lahko uporabimo za določitev lege protona v vodikovi vezi in nekaterih drugih strukturnih podatkov iz rezultatov meritev jedrske kvadrupolne resonance.